scientific data

OPEN

DATA DESCRIPTOR

3D+t Multifocal Imaging Dataset of Human Sperm

Fernando Montoya[1,7], Andrés Bribiesca-Sánchez[1,2,7], Paul Hernández-Herrera[3,7], Dan Sidney Díaz-Guerrero[1], Ana Laura Gonzalez-Cota[4], Hermes Bloomfield-Gadelha[5], Alberto Darszon[6] & Gabriel Corkidi[1]✉

Understanding human fertility requires dynamic and three-dimensional (3D) analysis of sperm movement, which extends beyond the capabilities of traditional datasets focused primarily on two-dimensional sperm motility or static morphological characteristics. To address this limitation, we introduce the 3D+t Multifocal Imaging Dataset of Human Sperm (3D-SpermVid), a repository comprising 121 multifocal video-microscopy hyperstacks of freely swimming sperm cells, incubated under non-capacitating conditions (NCC) and capacitating conditions (CC). This collection enables detailed observation and analysis of 3D sperm flagellar motility patterns over time, offering novel insights into the capacitation process and its implications for fertility. Data were captured using a multifocal imaging (MFI) system based on an optical microscope equipped with a piezoelectric device that adjusts focus at various heights, recording sperm movement in a volumetric space. By making this data publicly available, we aim to enable applications in deep learning and pattern recognition to uncover hidden flagellar motility patterns, fostering significant advancements in understanding 3D sperm morphology and dynamics, and developing new diagnostic tools for assessing male fertility, as well as assisting in the self-organizaton mechanisms driving spontaneous motility and navigation in 3D.

Background & Summary

Human spermatozoa are highly specialized cells with the single purpose of reaching and fertilizing the oocyte. Their ability to navigate the intricate 3D space of the female reproductive tract is critical to this task. Traditional studies often employ two-dimensional or simplified models to describe sperm motility, which, while useful for foundational insights, may not fully capture the rapid, irregular, and complex three-dimensional movements of both the head and flagellum[1]. Hence a realistic analysis of sperm swimming behavior must take into account both its movement in 3D and its changes over time.

A fundamental aspect of analyzing sperm motility is the quantitative description of movement patterns and the identification of different motility types[2–4]. Capacitation, a pivotal biological process, marks the sperm's final maturation steps, preparing it for potential fertilization. Approximately 10-20% of human sperm incubated under capacitating conditions exhibit hyperactivation, characterized by complex and asymmetrical flagellar beating[5]. Identifying hyperactivated sperm can be challenging, as their motility patterns are inherently irregular and dynamic. However, this motility pattern is essential for fertilization. Therefore, providing image sequences that accurately capture the 3D motility patterns of human sperm in NCC and CC contributes to the development of models to identify hyperactivated sperm, which is crucial to improve fertility assessments[2].

Recent advances in sperm analysis have been significantly supported by the development and availability of various image datasets, each offering unique insights into sperm morphology and motility[6,7]. These datasets range from high-resolution images categorizing sperm based on structural characteristics to sophisticated video

[1]Laboratorio de Imágenes y Visión por Computadora, Departamento de Ingeniería Celular y Biocatálisis, Instituto de Biotecnología, Universidad Nacional Autónoma de México, Cuernavaca, Morelos, México. [2]Posgrado en Ciencia e Ingeniería de la Computación, Universidad Nacional Autónoma de México, CDMX, Ciudad de México, México. [3]Facultad de Ciencias, Universidad Autónoma de San Luis Potosí, San Luis Potosi, SLP, México. [4]Universidad Autónoma Benito Juárez de Oaxaca, Oaxaca, México. [5]School of Engineering Mathematics and Technology & Bristol Robotics Laboratory, University of Bristol, BS8 1UB, Bristol, UK. [6]Departamento de Genética del Desarrollo y Fisiología Molecular, Instituto de Biotecnología, Universidad Nacional Autónoma de Mexico, Cuernavaca, Morelos, México. [7]These authors contributed equally: Fernando Montoya, Andrés Bribiesca-Sánchez, Paul Hernández-Herrera. ✉e-mail: gabriel.corkidi@ibt.unam.mx

recordings that capture the dynamic nature of sperm movement. Sperm morphology analysis has been significantly enhanced by a collection of datasets emphasizing 2D structural characteristics. The HSMA-DS dataset by Ghasemian *et al.*[6] and its derivative, the MHSMA dataset[8], collectively offer nearly 3,000 images, classifying sperm based on various abnormalities in the head and tail and providing a robust basis for automated morphological analysis. Complementarily, the HuSHEM and SCIAN-MorphoSpermGS datasets delve into the morphology of the sperm head, flagellum, vacuole and acrosome as means of classification[9,10]. The SMIDS dataset further broadens the scope with 3,000 images aimed at improving feature detection[11]. Additionally, McCallum *et al.*[12] contribute to this field with a dataset of 1,064 bright-field images, exploring the correlation between sperm morphology and genetic integrity. Together, these datasets offer a comprehensive view of sperm morphology through static images, laying the groundwork for advanced morphological studies despite their limited ability to capture the dynamic movement of sperm, which is fundamental in the cell's capacity to reach and fertilize the egg.

CASA systems have been the gold standard method in assessing 2D sperm motility[13]. These systems allow tracking the heads of a sample of sperm swimming in a volume with a restricted height during short time intervals and obtaining features describing its motility parameters. More recent methods have enabled the detection of not only the head movement, but also the 2D flagellar dynamics, which are the source of the sperm motility and as such can provide a deeper understanding of the sperm's behavior. In this direction, the VISEM-Tracking dataset by Thambawita *et al.*[14] introduces 20 video recordings of freely-swimming human sperm, coupled with manually annotated head bounding-box coordinates, providing a detailed view of sperm movement in 2D. Saggiorato *et al.*[7], collected a 2D+t centerline dataset, which was useful to identify flagellar beating frequencies related to the propulsion and steering of sperm, albeit within the constraints of two-dimensional analysis.

A 3D+t analysis can provide more accurate observations of sperm motility, however collecting and analyzing such data is a challenging task. Venturing into this realm, Bukatin *et al.*[15] used darkfield microscopy with a Rayleigh-Sommerfeld approximation -which estimates the z-coordinate from the defocusing- to capture the 3D coordinates of the sperm flagellum. Dardikman-Yoffe *et al.*[16] leveraged off-axis holographic microscopy to capture 3D human sperm movements. Subsequently, Gong *et al.*[17] utilized digital inline holographic microscopy, achieving a capture rate of 1,000 fps to observe 14 human sperm samples. Notably, imaging techniques for 3D+t sperm acquisition involve complex methods for deriving 3D data from a 2D image. 3D+t datasets often contain the flagellum coordinates, but not the raw video data. This approach, while innovative, limits the potential for comprehensive analysis that could benefit from accessing the original high-resolution, temporal sequences.

To facilitate the 3D analysis of human sperm dynamics, we generated the 3D+t Multifocal Imaging Dataset of Human Sperm (3D-SpermVid)[18–29], which contains 121 multifocal video-microscopy hyperstacks, each recorded over 1–3.5 seconds. This dataset includes sperm incubated under NCC and CC conditions, enabling the study of motility under these experimental condition.

As the first publicly available collection of 3D+t raw multifocal videomicroscopy acquisitions of sperm dynamics, the 3D-SpermVid dataset surpasses prior datasets that focus on static morphology or limited kinetic analysis by enabling detailed observation of movement in three dimensions over time[18–29].

The dataset is particularly well-suited for applications such as:

- Studies of 3D sperm motility[2,30], and flagellar beating and molecular motor self-organization,
- Development and testing of image analysis algorithms,
- Research in reproductive health diagnostics,
- Machine learning tasks, including training convolutional neural networks to analyze multidimensional imaging data.
- Next generation of CASA systems,
- Model fitting with experiments, and data driven modeling, and
- As support for a variety of cell biology and biophysics applications.

This dataset provides a valuable resource for exploring sperm dynamics under varying conditions and supports diverse computational and biological research. By identifying 3D motility patterns in NCC and CC, the 3D-SpermVid dataset has the potential to advance diagnostic tools and treatments, significantly impacting scientific and clinical fields.

Methods

Consent & ethical approval. Sperm samples were obtained from young healthy donors by masturbation. The donors were carefully informed and gave their written consent under the supervision and approval (approval number 469) of the Bioethics Committee of the Instituto de Biotecnología, UNAM. The informed consent form explicitly states that donors agree to disclose their data, while ensuring their identity remains anonymous.

The cells used in the study were selected from semen samples that met the World Health Organization (WHO) standards[31].

Sperm preparations. As an experimental control, 49 samples were placed in non-capacitating media, and 72 in capacitating media to enable their hyperactivated motility since only capacitated sperm cells can show signs of hyperactivated motility. Highly motile cells were recovered from semen samples through a swim-up separation after incubation for 1 hour in HTF medium at 37 $^{\circ}$C in a humidified chamber with 5% CO_2 concentration. Once recovered, cells were centrifuged for 5 minutes at 3000 rpm.

For the non-capacitated condition, the samples were resuspended in physiological media consisting of 94 mM NaCl, 4 mM KCl, 2 mM $CaCl_2$, 1 mM $MgCl_2$, 1 mM Na pyruvate, 5 mM glucose, 30 mM HEPES, and 10

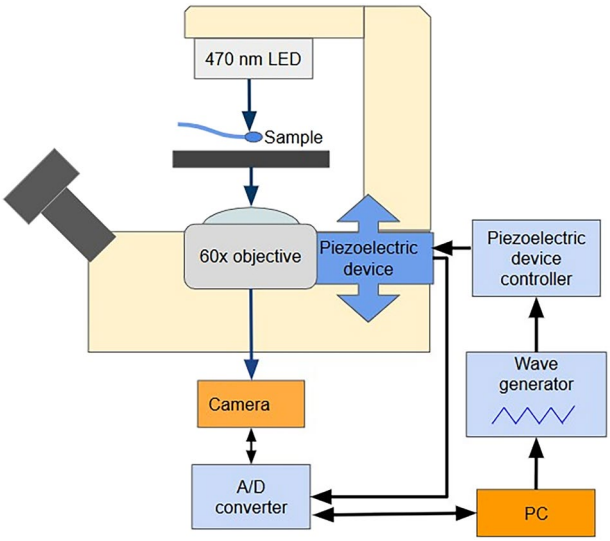

Fig. 1 Experimental device block diagram. The experimental device is comprised of an inverted microscope with a piezoelectric device that allows the vertical oscillation of the objective, guided by a wave generator, controlled by piezoelectric device controller, while a camera records images. An A/D converter controls the camera and digitizes the piezo and camera signals to record the *z*-position of the objective every time a picture was taken[32,35].

mM lactate at pH 7.4. For the capacitated condition, 5 mg/ml of Bovine Serum Albumin and 2 mg/ml $NaHCO_3$ was added to the non-capacitating media.

From each semen sample, 500 microliters with a concentration of 10^2 cells per milliliter were placed in an imaging chamber, and then individual cells were manually focused and selected for recording using the platen's knobs. The temperature of the samples was maintained at 37 °C with a thermal controller (Warner Instruments, TCM/CL100).

Experimental setup and multifocal hyperstack acquisition. The image sequences were obtained using an updated version of the MFI setup reported in[32], illustrated in Fig. 1. The acquisition was performed using an inverted Olympus IX71 microscope placed on an optical table [TMC (GMP SA, Switzerland)]. A 60X water immersion objective with N.A. = 1.00 (Olympus UIS2 LUMPLFLN 60X W) was attached to a piezoelectric device P-725 (Physik Instruments, MA, USA) mounted on the microscope. This device allows the objective to displace along the *z*-axis while a high-speed camera records images of the sample. The piezoelectric device, together with the objective, oscillated at a frequency of 90 Hz and an amplitude of 20 μm. A servo-controller E501 via a high-current amplifier E-55 (Physik Instruments, MA, USA) was used to fine-tune the piezoelectric oscillations. A MEMRECAM Q1v high-speed camera (NAC, U.S.A.) with 8 GB internal storage was set to record at 5000-8000 fps with a resolution of 640 × 480 pixels. At this speed and resolution, the camera was able to record up to 5.5-3.5 seconds respectively.

A NI USB-6211 digital/analog converter (National Instruments, USA) was used to digitize the camera and piezoelectric device signals, making it straightforward to determine the height at which each image was recorded, since the camera signal indicates when each picture was taken and the piezoelectric signal is directly proportional to the piezo-objective height. A custom-developed software application was written in C# to manage the acquisition, configuring and synchronizing the camera and piezoelectric device. After an experiment is triggered, this software produces a single text file with the height of each image.

Image sequences recorded while the piezoelectric device moved upwards were arranged into TIF image stacks. Image sequences recorded while the piezoelectric device was going downwards were discarded due to the hysteresis in the movement, to keep consistency in the focal planes. Each stack is made from image sequences of a sperm cell taken at different focal planes spanning a depth of 20 μm. This depth constitutes the *z*-axis, while the *XY* plane is given by the standard microscope acquisition, as shown in Fig. 2. The scale between microns and pixels is 1 px = 118/640 µm = 0.184375 µm. Thus, a TIF stack is the 3D image sequences representation of a given sperm at a given time. The *xyz* TIF stacks are concatenated into a 4D (3*D* + t) *TIF hyperstack*. This configuration facilitates exploring the recorded volume in both space and time, as well as the application of image filters and computations along these axes using suitable image processing software, such as ImageJ[33]. Using these hyperstacks the spatio-temporal motility patterns can be analyzed for the different cells considered over both experimental conditions: NCC and CC.

Data Records

The 3D-SpermVid dataset is divided into 12 repositories available at Zenodo[18–29], as shown in Table 1. This dataset comprises 121 high-speed, three-dimensional image sequences (3D+t TIF hyperstacks) of freely swimming sperm cells, with a total size of 272 GB. Each hyperstack consists of images with a resolution of 640 × 480 pixels. The hyperstacks consist of 29 to 45 focal planes (for 5000-8000 fps respectively), covering a total depth of

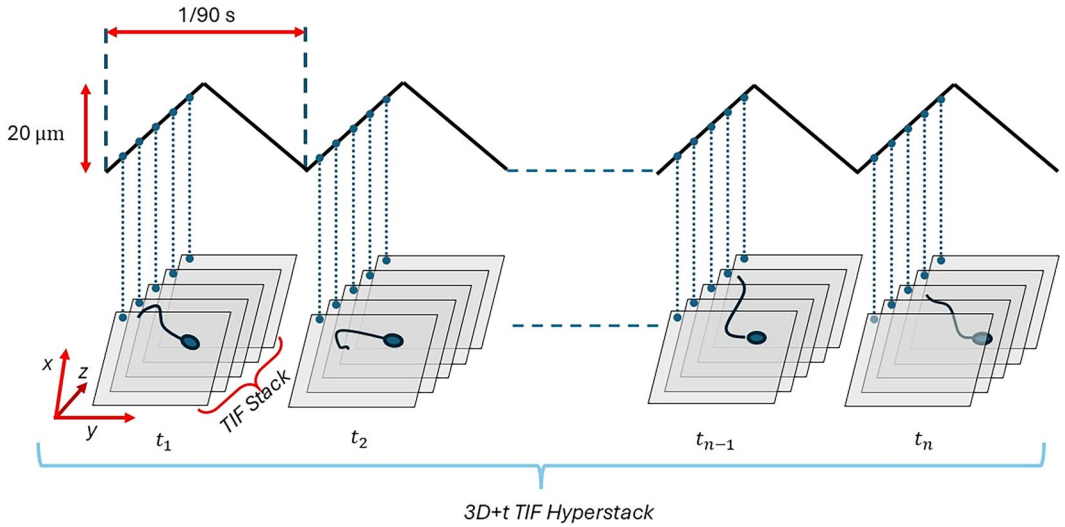

Fig. 2 Spatio-temporal acquisition of 3D+t TIF stacks in Sperm Motility Analysis. The objective oscillates at a 90 Hz frequency and 20 μm amplitude, driven by a piezoelectric device. A 3D TIF stack consists of the images recorded as the piezoelectric device moves from the bottom to the top. Image sequences recorded while the piezoelectric device was going downwards were discarded due to the hysteresis in the movement, to keep consistency in the focal planes. The x, y, and z axes indicate the spatial orientation of the image stacks. Each individual stack contributes to the formation of a 3D+t TIF hyperstack over the elapsed time, providing a detailed three-dimensional view of sperm motility patterns crucial for understanding capacitation dynamics.

DOI	Number of cells	Date	Type
https://doi.org/10.5281/zenodo.11222052[18]	17	2021-07-30	NCC
https://doi.org/10.5281/zenodo.11200343[19]	17	2021-07-04	NCC
https://doi.org/10.5281/zenodo.10944023[20]	15	2021-07-02	NCC
https://doi.org/10.5281/zenodo.11264343[21]	8	2019-03-26	CC
https://doi.org/10.5281/zenodo.11254480[22]	4	2018-10-31	CC
https://doi.org/10.5281/zenodo.11248030[23]	11	2018-10-30	CC
https://doi.org/10.5281/zenodo.11244698[24]	11	2018-10-26	CC
https://doi.org/10.5281/zenodo.11238481[25]	6	2017-11-08	CC
https://doi.org/10.5281/zenodo.11238630[26]	8	2017-08-15	CC
https://doi.org/10.5281/zenodo.11237174[27]	4	2017-06-07	CC
https://doi.org/10.5281/zenodo.11238009[28]	7	2017-06-02	CC
https://doi.org/10.5281/zenodo.11224072[29]	13	2017-06-01	CC

Table 1. Summary of the 3D-SpermVid dataset[18–29].

$20 \pm 2\,\mu$m. This slight variation arises from inertia during the piezoelectric device's movement. The average gap between adjacent focal planes is 0.69-0.45 μm for 5000-8000 fps respectively. Each experiment lasted between 1 and 3.5 seconds, corresponding to 90–315 time frames. The dataset includes both NCC and CC sperm cells, providing a comprehensive resource for studying sperm motility and the capacitation process.

It is important to point out that cells incubated in CC do not necessarily capacitate, though, only around 10–20% hyperactivate[2,5,34]. This dataset contains raw data based solely on incubation conditions, without any pre-classified cells. Further classification procedures are necessary to establish this distinction with certainty. The 3D-SpermVid dataset serves as a valuable resource of 3D data, enabling the testing and validation of various classification algorithms for hyperactivated sperm, such as the one described in *Hernández et al.*[2].

The NCC dataset includes 49 recorded cells[18–20], while the CC dataset has 72[21–29], as sperm incubated in CC exhibit broader behavioral dynamics. As mentioned, since only a minor group of cells incubated in capacitating media become truly hyperactivated (i.e., fully capacitated)[2,5,34], we believe it is crucial to include a larger number of these cells. In contrast, cells incubated in non-capacitating media serve as controls exhibiting lower variability.

Dataset Folder Structure. The 3D-SpermVid dataset is comprised of 121 cell recordings, 49 belonging to the NCC sperm, and 72 belonging to the CC sperm[18–29]. Due to the large volume of data, the dataset has been divided into 12 repositories, each corresponding to a date of acquisition where sperm were either incubated in NCC or CC (see Table 1). Each repository contains between 4 and 17 TIF hyperstacks, along with an acquisition metadata file TXT and a CSV file recording the height of each image. Each row in the CSV file corresponds to the

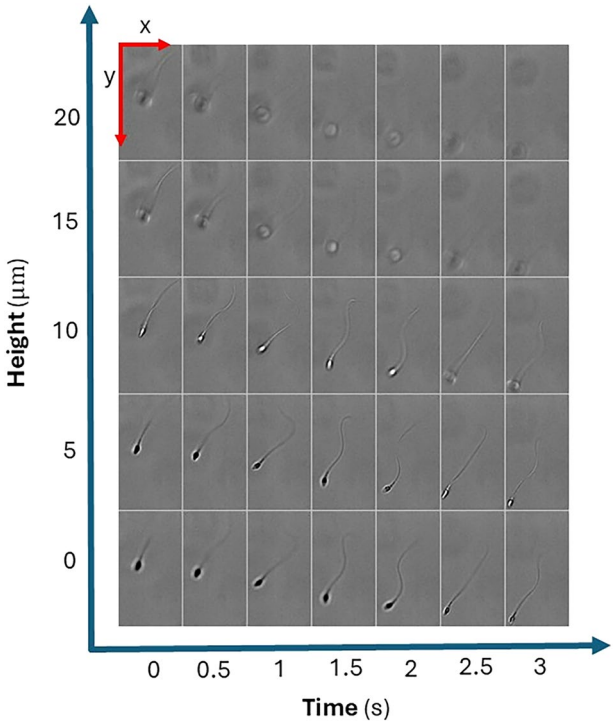

Fig. 3 Sample montage of a 3D+t hyperstack. The hyperstack features 45 focal planes at 90 frames per second; this montage displays sperm dynamics across five selected focal planes (at heights of approximately 0, 5, 10, 15, and 20 μm) over a 3-second span. Note that the flagellar beat is non-planar, with the flagellum frequently appearing in focal planes above or below the sperm head. The visualization emphasizes the spatial and temporal range of the dataset.

height of an image in the hyperstack, and each column represents the height values at a specific time point. The files for each experiment are titled respectively as follows:

- Sperm-(CELLNUMBER)-(NCC/CC)_(DATE)_Exp(NUMBER).tif
- Sperm-(CELLNUMBER)-(NCC/CC)_(DATE)Exp(NUMBER)_info.txt
- z-axis-values-(DATE)-Exp(NUMBER).csv

For example, the files for one of the experiments in the 2021/07/30 dataset[18] are titled:

- Sperm-1-NoCap_210730_Exp4.tif
- Sperm-1-NoCap_210730_Exp4_info.txt
- z-axis-values-210730-Exp4.csv

Note that in the filenames, "NoCap" corresponds to NCC, and "Cap" corresponds CC.

Figure 3 presents a montage of selected focal planes and time points from a 3D+t hyperstack of a non-capacitated sperm cell. This figure highlights the structure and complexity of the recorded data, offering a visual representation of sperm motility captured in the dataset.

The size and detail of the three-dimensional video-microscopy hyperstacks in the 3D-SpermVid dataset[18–29] makes it a unique source of human sperm information. Moreover, the added stacks and hyperstacks allow novel qualitative explorations that could become the start of new sperm motility research. The 3D-SpermVid dataset[18–29] enables: analysis of NCC sperm swimming oriented to characterize basal spermatozoa three-dimensional movement; examination of CC spermatozoa to identify their spatiodynamical characteristics and the distribution of swimming characteristics among cells of the sample.

These 3D acquisitions have allowed us to explore the 3D flagellar beat of activated and hyperactivated human sperm, as well as analyzing cell rotation along the axis of movement[2,30,35,36]. We believe that making the data publicly accessible will facilitate the exploration of the 3D motion patterns of human sperm.

In summary, the 3D-SpermVid dataset[18–29] provides a comprehensive dataset for studying sperm motility in 3D over time, offering valuable insight into the dynamical behaviors of sperm cells under two physiologically important experimental conditions. The dataset is well organized, with detailed metadata accompanying each hyperstack, ensuring that it is accessible and useful for a wide range of research applications in fertility and reproductive health.

Technical Validation

All hyperstacks were manually curated to ensure that each focal plane was reconstructed accurately. This process began with a careful inspection of the raw image sequences to confirm that no artifacts or inconsistencies were present that might affect the quality of the reconstructed 3D+t hyperstacks. Next, a visual check was conducted to ensure that the focus of each image matched the focus at the same height in the subsequent frame, verifying the synchronization between the piezoelectric device and the camera. If the signals were found to be out of phase, this was corrected by skipping images (usually only one was enough) to ensure precise synchronization. Furthermore, the force of the fast vibration of the piezoelectric device can introduce some movement in the XY plane. This drift was corrected using ImageJ's StackReg plugin[33], ensuring alignment. In addition to manual curation and visual validation, we performed quantitative checks on the metadata to ensure that all acquisition parameters were correctly recorded and consistent with the experimental setup. This included verifying the heights at which images were captured and confirming the frame rates and resolutions used during acquisition.

This data descriptor is linked to Version 1 (V1) of the datasets[18–29], which have undergone peer review alongside the manuscript. The DOIs cited in the text refer exclusively to V1. Any future updates to the data will be released as a separate version with a new DOI. Since these subsequent versions will not undergo the same peer review process, they will not be covered by this data descriptor. However, we remain committed to ensuring the accuracy and reliability of any new data through rigorous validation. Users are encouraged to provide feedback if any issues are identified, and we will address them promptly to uphold the highest quality standards. This rigorous validation supports the dataset's use in a wide range of research applications, from basic biological studies, to mathematics and biophysics and clinical diagnostics in reproductive health.

Usage Notes

The TIF hyperstacks in the dataset are 4D images (t,z,y,x). To be able to observe and process each dimension of the TIF file we recommend installing ImageJ (v1.54p)[33], a widely-used open-source tool for image analysis. After downloading a TIF file from the 3D-SpermVid repositories[18–29], one can drag and drop it on the ImageJ GUI to load it with the stack Viewer, which allows scrolling along the z and t dimensions of the TIF file, as shown in the guide: https://imagej.net/ij/docs/guide/146-8.html. Tools are available to manage and process the stack in the "Image > Stacks" and "Image > Hyperstacks" menu, and they are described thoroughly in the documentation[33].

For more customizable processing workflows, including training and testing neural networks, Python's scikit-image library can be used to load the hyperstack as a 4D array[37].

Code availability

The code for constructing and processing the TIF hyperstacks is openly accessible in the following GitHub repository: https://github.com/paul-hernandez-herrera/LIVC_UNAM/tree/main/matlab_code/Sperm_tracing_3D_Release.

Received: 2 January 2025; Accepted: 9 May 2025;
Published online: 18 May 2025

References

1. Powar, S. *et al.* Unraveling the kinematics of sperm motion by reconstructing the flagellar wave motion in 3D. *Small Methods* **6**, 2101089, https://doi.org/10.1002/smtd.202101089 (2022).
2. Hernández, H. O. *et al.* Feature-based 3D+t descriptors of hyperactivated human sperm beat patterns. *Heliyon* **10**, e26645, https://doi.org/10.1016/j.heliyon.2024.e26645 (2024).
3. Ooi, E. H. *et al.* The mechanics of hyperactivation in adhered human sperm. *R. Soc. Open Sci.* **1**, 140230, https://doi.org/10.1098/rsos.140230 (2014).
4. Nassir, M., Levi, M. & Shaked, N. T. Dynamic 3D modeling for human sperm motility through the female cervical canal and uterine cavity to predict sperm chance of reaching the oocyte. *Cells* **12**, 203, https://doi.org/10.3390/cells12010203 (2023).
5. Suarez, S. S. Control of hyperactivation in sperm. *Hum. Reprod. Update* **14**, 647–657, https://doi.org/10.1093/humupd/dmn029 (2008).
6. Ghasemian, F. *et al.* An efficient method for automatic morphological abnormality detection from human sperm images. *Comput. Methods Programs Biomed.* **122**, 409–420, https://doi.org/10.1016/j.cmpb.2015.08.013 (2015).
7. Saggiorato, G. *et al.* Human sperm steer with second harmonics of the flagellar beat. *Nat. Commun.* **8**, 14191, https://doi.org/10.1038/ncomms14191 (2017).
8. Javadi, S. & Mirroshandel, S. A. A novel deep learning method for automatic assessment of human sperm images. *Comput. Biol. Med.* **109**, 182–194, https://doi.org/10.1016/j.compbiomed.2019.04.030 (2019).
9. Shaker, F. *et al.* A dictionary learning approach for human sperm heads classification. *Comput. Biol. Med.* **91**, 181–190, https://doi.org/10.1016/j.compbiomed.2017.10.009 (2017).
10. Chang, V., Garcia, A., Hitschfeld, N. & Härtel, S. Gold-standard for computer-assisted morphological sperm analysis. *Comput. Biol. Med.* **87**, 143–158, https://doi.org/10.1016/j.compbiomed.2017.03.004 (2017).
11. Ilhan, H. O. & Serbes, G. Sperm morphology analysis by using the fusion of two-stage fine-tuned deep networks. *Biomed. Signal Process. Control* **71**, 103246, https://doi.org/10.1016/j.bspc.2021.103246 (2022).
12. McCallum, C. *et al.* Deep learning-based selection of human sperm with high DNA integrity. *Commun Biol.* **2**, 250, https://doi.org/10.1038/s42003-019-0491-6 (2019).
13. Finelli, R. *et al.* The validity and reliability of computer-aided semen analyzers in performing semen analysis: a systematic review. *Transl. Androl. Urol.* **10**, 3069–3079, https://doi.org/10.21037/tau-21-276 (2021).
14. Thambawita, V. *et al.* VISEM-Tracking, a human spermatozoa tracking dataset. *Sci. Data* **10**, 260, https://doi.org/10.1038/s41597-023-02173-4 (2023).
15. Bukatin, A. *et al.* Bimodal rheotactic behavior reflects flagellar beat asymmetry in human sperm cells. *Proc. Natl Acad. Sci. USA* **112**, 15904–15909, https://doi.org/10.1073/pnas.1515159112 (2015).
16. Dardikman-Yoffe, G. *et al.* High-resolution 4-D acquisition of freely swimming human sperm cells without staining. *Sci. Adv.* **6**, eaay7619, https://doi.org/10.1126/sciadv.aay7619 (2020).

17. Gong, A. *et al*. Reconstruction of the three-dimensional beat pattern underlying swimming behaviors of sperm. *Eur. Phys. J. E* https://doi.org/10.1140/epje/s10189-021-00076-z (2021).
18. Montoya, F. *et al*. 3D+t freely swimming human sperm incubated in Non-Capacitating Conditions (NCC) 2021-07-30. *Zenodo* https://doi.org/10.5281/zenodo.11222052 (2025).
19. Montoya, F. *et al*. 3D+t freely swimming human sperm incubated in Non-Capacitating Conditions (NCC) 2021-07-04. *Zenodo* https://doi.org/10.5281/zenodo.11200343 (2025).
20. Montoya, F. *et al*. 3D+t freely swimming human sperm incubated in Non-Capacitating Conditions (NCC) 2021-07-02. *Zenodo* https://doi.org/10.5281/zenodo.10944023 (2025).
21. Montoya, F. *et al*. 3D+t freely swimming human sperm incubated in Capacitating Conditions (CC) 2019-03-26. *Zenodo* https://doi.org/10.5281/zenodo.11264343 (2025).
22. Montoya, F. *et al*. 3D+t freely swimming spermatozoa incubated in Capacitating Conditions (CC) 2018-10-31. *Zenodo* https://doi.org/10.5281/zenodo.11254480 (2025).
23. Montoya, F. *et al*. 3D+t freely swimming spermatozoa incubated in Capacitating Conditions (CC) 2018-10-30. *Zenodo* https://doi.org/10.5281/zenodo.11248030 (2025).
24. Montoya, F. *et al*. 3D+t freely swimming spermatozoa incubated in Capacitating Conditions (CC) 2018-10-26. *Zenodo* https://doi.org/10.5281/zenodo.11244698 (2025).
25. Montoya, F. *et al*. 3D+t freely swimming spermatozoa incubated in Capacitating Conditions (CC) 2017-11-08. *Zenodo* https://doi.org/10.5281/zenodo.11238481 (2025).
26. Montoya, F. *et al*. 3D+t freely swimming spermatozoa incubated in Capacitating Conditions (CC) 2017-08-15. *Zenodo* https://doi.org/10.5281/zenodo.11238630 (2025).
27. Montoya, F. *et al*. 3D+t freely swimming spermatozoa incubated in Capacitating Conditions (CC) 2017-06-07. *Zenodo* https://doi.org/10.5281/zenodo.11237174 (2025).
28. Montoya, F. *et al*. *3D+t freely swimming spermatozoa incubated in Capacitating Conditions (CC) 2017-06-02* [Dataset]. Zenodo https://doi.org/10.5281/zenodo.11238009 (2025).
29. Montoya, F. *et al*. 3D+t freely swimming human sperm incubated in Capacitating Conditions (CC) 2017-06-01. *Zenodo* https://doi.org/10.5281/zenodo.11224072 (2025).
30. Bribiesca-Sánchez, A. *et al*. A three-dimensional extension of the slope chain code: analyzing the tortuosity of the flagellar beat of human sperm. Pattern Anal Applic 27, 74 https://doi.org/10.1007/s10044-024-01286-9 (2024).
31. World Health Organization. WHO laboratory manual for the examination and processing of human semen. (2021).
32. Corkidi, G., Taboada, B., Wood, C. D., Guerrero, A. & Darszon, A. Tracking sperm in three-dimensions. *Biochem. Biophys. Res. Commun*. https://doi.org/10.1016/j.bbrc.2008.05.189 (2008).
33. Rueden, C. T. *et al*. *ImageJ2: ImageJ for the next generation of scientific image data*. *BMC Bioinformatics* https://doi.org/10.1186/s12859-017-1934-z (2017).
34. Cohen-Dayag, A., Tur-Kaspa, I., Dor, J., Mashiach, S. & Eisenbach, M. Sperm capacitation in humans is transient and correlates with chemotactic responsiveness to follicular factors. *Proc. Natl. Acad. Sci. USA* https://doi.org/10.1073/pnas.92.24.11039 (1995).
35. Corkidi, G. *et al*. Human sperm rotate with a conserved direction during free swimming in four dimensions. *J. Cell Sci*. https://doi.org/10.1242/jcs.261306 (2023).
36. Ren, X. *et al*. Fluid flow reconstruction around a free-swimming sperm in 3D. *bioRxiv* https://doi.org/10.1101/2024.05.29.596379 (2024).
37. van der Walt, S. *et al*. scikit-image: image processing in Python. *PeerJ* https://doi.org/10.7717/peerj.453 (2014).

Acknowledgements

This work was supported by DGAPA PAPIIT (IN105222 to GC and IN200919 to AD), and SECIHTI (PhD scholarship to ABS and CF-2023-I-291 to AD), and Chan-Zuckerberg Initiative (DAF Grant Number 2023-329644, an advised fund of Silicon Valley Community Foundation) to PHH. We thank Paulina Torres Rodríguez for her valuable technical support to the project.

Author contributions

Conceptualization: F.M., A.B-S., P.H-H., D.S.D-G., H.B.-G., A.D., G.C.; Methodology: F.M., A.B-S., P.H-H., A.L.G.-C., A.D., G.C.; Software: F.M., A.B-S, P.H.-H.,D.S.D-G.; Validation: F.M., A.B-S, P.H.-H., D.S.D-G., G.C.; Resources: G.C., A.D.; Writing - original draft: A.B-S., F.M., D.S.D-G., G.C.; Writing - review & editing: A.B-S., F.M., P.H-H., D.S.D-G., A.L.G.-C., H.B.-G., A.D., G.C.; Project administration: G.C., A.D.; Funding acquisition: G.C., A.D.

Competing interests

The authors declare no competing interests.

Additional information

Correspondence and requests for materials should be addressed to G.C.

Reprints and permissions information is available at www.nature.com/reprints.

Publisher's note Springer Nature remains neutral with regard to jurisdictional claims in published maps and institutional affiliations.